A structure preserving scheme for the Kolmogorov–Fokker–Planck equation

Erich L. Foster [a], Jérôme Lohéac [b,*], Minh-Binh Tran [c]

[a] *Sandia National Laboratories, Center for Computing Research, P.O. Box 5800, Albuquerque, NM 87185-1321, USA*
[b] *LUNAM Université, IRCCyN UMR CNRS 6597 (Institut de Recherche en Communications et Cybernétique de Nantes), École des Mines de Nantes, 4 rue Alfred Kastler, 44307 Nantes, France*
[c] *Department of Mathematics, University of Wisconsin Madison, USA*

A R T I C L E   I N F O

A B S T R A C T

In this paper we introduce a numerical scheme which preserves the behavior of solutions to the Kolmogorov Equation as time tends to infinity. The method presented is based on a self-similar change of variables technique to transform the Kolmogorov Equation into a new form, such that the problem of designing structure preserving schemes, for the original equation, amounts to building a standard scheme for the transformed equation. This transformation also has the added benefit of allowing for an exact operator splitting scheme, whereas in the original form a standard operator splitting was only second-order. Finally, we verify the preservation of long time behavior through numerical simulations.

© 2016 Elsevier Inc. All rights reserved.

1. Introduction

In this paper we are concerned with preserving the long time behavior of numerical solutions of the Kolmogorov Equation

$$\partial_t f - \partial_v^2 f - v \partial_x f = 0 \,. \tag{1}$$

The hypoellipticity and the asymptotic behavior of this operator are well known, see for instance the original work of L. Hörmander [17] and the work of C. Villani [25] and F. Rossi [23]. The solution of eq. (1) over all of $\mathbb{R}^2$ is known to decay polynomially in time, while the solution on a truncated domain, $\Omega \subset \mathbb{R}^2$, is known to decay exponentially in time in L^2 norm, with periodic boundary condition.

Attempting to simulate over all of $\mathbb{R}^2$ can be quite expensive and complicated, thus simulating over a truncated domain is quite attractive in this sense. However, as stated, the asymptotic behavior on a truncated domain is quite different from the asymptotic behavior on all $\mathbb{R}^2$. When simulating over a truncated domain, a set of artificial boundary conditions must be chosen. These boundary conditions then interact with the solution, such that the asymptotic behavior is changed. In this paper we present a scheme for solving the Kolmogorov Equation, eq. (1), on a truncated domain, $\Omega \subset \mathbb{R}^2$, which preserves the long time behavior of the solution to the Kolmogorov Equation over the whole space, $\mathbb{R}^2$.

To our knowledge, only a few papers investigate the long time asymptotics for numerical solutions of Fokker–Planck type equations. One of most popular schemes for Fokker–Planck equations of type

---

* Corresponding author.
E-mail addresses: elfost@sandia.gov (E.L. Foster), jerome.loheac@irccyn.ec-nantes.fr (J. Lohéac), mtran23@wisc.edu (M.-B. Tran).

$$\partial_t u(x) = \frac{1}{M(x)} \operatorname{div}(N(x) \nabla u(x) + P(x)u(x))$$

is the Chang–Cooper method [9], which is a finite difference scheme in both space and time. The Chang–Cooper method was developed in [6] and [21]. In [3], [4] and [8], the authors studied nonlinear Fokker–Planck equations, where the nonlinearity is on the diffusion term. Systems of Fokker–Planck type equations have also been studied in [12] and [16] by a Voronoi finite volume discretization.

However, most of the equations studied before possess full parabolic structures, and thus the existing approaches aren't appropriate for the Kolmogorov equation, which has a different structure: there is an advection term but no diffusion term in the x-variable. As can be seen from its form, the solution of the equation not only diffuses in the direction of v, by the effect of the diffusion operator ∂_v^2, but also in the direction of x, due to the transport equation $\partial_t f - v \partial_x f$. This diffusion process causes the support of the solution to grow over time and therefore the artificial boundary conditions become quite important over time.

For the Kolmogorov Equation, one may choose one of two natural approaches to solving the Kolmogorov equation numerically; either by an operator splitting method or by a change of variables. The most natural operator splitting technique to use is one by which the Kolmogorov Equation is split into two equations: a transport and a heat equation. In order to solve the heat equation by some discretization method, one needs to restrict the domain $\mathbb{R}^2$ to a truncated domain and impose boundaries condition. However, it is known that the support of the solution to the heat equation spreads to the whole space as time evolves, therefore restricting the computational domain to a truncated domain is not an ideal strategy to observe the long time behavior of the solution of eq. (1).

On the other hand the change of variables

$$f(t, v, x) = g(t, v, x + tv) = g(t, v, z) \tag{2}$$

transforms the Kolmogorov Equation, eq. (1), into

$$\partial_t g = \partial_v^2 g + 2t \partial_{vz} g + t^2 \partial_z^2 g. \tag{3}$$

With this change of variables the frame of reference follows the transport and this allows one to apply classical techniques such as the finite element method (FEM). However, the support of the solution spreads to the whole space as time evolves. In Section 4, we prove that for a truncated domain, the solutions of eq. (1) and eq. (3) set in a bounded domain with homogeneous Dirichlet boundary conditions converge exponentially to zero, while the solution to the original problem converges to zero in polynomial order.

Inspired by the self-similarity technique in control theory (see for instance [10,11]), we propose, in Section 3, a new strategy to design structure preserving schemes for the Kolmogorov Equation by using the technique of self-similarity change of variables. This scheme has the benefit of preserving the polynomial decay expected from a solution obtained over the whole space $\mathbb{R}^2$, but allowing us to solve eq. (1) on a truncated domain. Thus, simulations are more computationally efficient and less reliant on artificial boundary conditions.

We would also like to mention a similar technique: in [14,13], F. Filbet et al. introduce a new technique based on the idea of rescaling the kinetic equation according to hydrodynamic quantities. The rescaling in velocity, is as follows

$$f(t, x, v) = \frac{1}{\omega(t, x)^{d_v}} g\left(t, x, \frac{v}{\omega(t, x)}\right),$$

where the function ω is an accurate measure of the support of the function f and d_v is the dimension of the velocity variable v. The rescaling can be defined based on the information provided by the hydrodynamic fields, computed from a macroscopic model corresponding to the original kinetic equation. However, the collisional kinetic equations considered by F. Filbet et al. are much more sophisticated than the Kolmogorov Equation, since they are nonlinear. Therefore, the scaling in space $\omega(t, x)$ has to be computed through hydrodynamic quantities, while in our case, the space scale is quite simple to compute.

Our idea is quite similar to theirs, but goes further; we not only rescale the velocity variable, but also the time variable. Indeed, we rescale the time and space so that the solution of the rescaled equation converges to a non-zero steady state solution. This has the benefit of maintaining compact support, rather than an expansion of the solution to the whole space. Numerically, one can see with the time rescaling, as time evolves, the support of the self-similarity solution is trapped in a truncated domain if the initial condition is compactly supported.

Rescaling/self-similar algorithms are a well-known strategy in constructing numerical schemes, which can capture the profile of blow up solutions. Such algorithms were first introduced in [2] and have continued to be developed in [5,20,18, 24]. We refer to [22] for a different attempt in this direction, using a finite-difference centered approximation.

The structure of the paper is as follows: in Section 2, we recall some classical results on the kernel and asymptotic behavior of the solution of the Kolmogorov Equation. In Section 3, we introduce the self-similar formulation of the Kolmogorov Equation. We also provide a theoretical study on the solution of the self-similar equation: in Proposition 3.1 the solution is proven to converge to a steady state in Theorem 3.1. In Section 4, we discuss truncating the domain for the Kolmogorov Equation in three forms: the original form eq. (1), the Lagrangian form eq. (3) and the self-similar form eq. (5). We prove

that once the domain is truncated the solution to the original form eq. (1) and the Lagrangian form eq. (3) converge exponentially to zero, which does not correspond to the polynomial convergence predicted for the original Cauchy problem. For the self-similar case eq. (5), we will see numerically in Section 5 that the solution converges to a steady state. This coincides with the property of the original Cauchy problem. As a consequence, we choose to truncate and discretize the self-similar equation (5). The convergence of the truncated method is given in Proposition 4.2. We also give a necessary condition, eq. (12), which should be satisfied for the truncated domain in order to obtain a time asymptotic convergence to a steady state. In Section 5 we introduce our method for simulating the Kolmogorov Equation in a truncated domain for both the original form of the Kolmogorov Equation and the Self-Similar form of the Kolmogorov Equation. We use an operator splitting technique combined with a finite element method. The analysis of the operator splitting technique is given in Proposition 5.1. Furthermore, numerical results verifying the theory are presented in Section 6.

2. Kernel and long time behavior

In this section we recall the kernel for the Kolmogorov equation, on the whole space $\mathbb{R}^2$, and describe the long time behavior. This will be useful in determining the correctness of the methods developed in later sections and for developing the self-similarity change of variables.

The kernel is obtained by a standard method using the Fourier transform, and was originally obtained by A. Kolmogorov [19] in the '60s. Later a more general statement was developed by O. Calin, D.-C. Chang and H. Haitao [7], and in K. Beauchard and E. Zuazua [1].

Proposition 2.1. *The kernel of* (3) *is*

$$G_t(v, z) = \frac{\sqrt{3}}{2\pi t^2} e^{-\frac{1}{4t^3}(3z^2 + (2t\,v - 3z)^2)} \qquad (t > 0,\ x \in \mathbb{R},\ v \in \mathbb{R}). \tag{4}$$

Given the initial data, $f_0 \in C^\infty(\mathbb{R}^2)$*, the solution* $f(t, v, x)$ *to* (1) *is given by the convolution*

$$f(t, v, x) = (f_0 * G_t)(v, x + v\,t) \qquad (t > 0,\ x \in \mathbb{R},\ v \in \mathbb{R}).$$

In what follows, we will give precise decay rates, using the explicit form to the solution of (1) given in Proposition 2.1. Substituting $z = x + v\,t$ into (4) we see the kernel in (v, x) variables is

$$G_t(v, x + v\,t) = \frac{\sqrt{3}}{2\pi t^2} e^{-\frac{1}{4t^3}(3\,(x+t\,v)^2 + (3x+t\,v)^2)}.$$

Thus, the kernel represents a series of ellipses given by the Gaussian

$$e^{-\frac{1}{4t^3}(3\,(x+t\,v)^2 + (3x+t\,v)^2)},$$

where the spread of the ellipse in the direction $x + t\,v$ is described by the standard deviation $\frac{2t^{\frac{3}{2}}}{\sqrt{3}}$, on the other hand the spread in the direction $3x + t\,v$ is described by the standard deviation $2t^{\frac{3}{2}}$. Thus, we see not only that the shape changes over time, but the width of the solution changes over time, and it changes to a varying degree in different directions.

Now we want to know what the behavior of the solution of (1) is as $t \to \infty$. To this end, we compute the asymptotic behavior of the Kernel G.

Lemma 2.1. *For every* $q \in [1, \infty]$ *and every* $t > 0$*, we have* $G_t \in L^q(\mathbb{R}^2)$ *and*

$$\|G_t\|_{L^q(\mathbb{R}^2)} = \begin{cases} q^{\frac{-1}{q}} \left(\dfrac{\sqrt{3}}{2\pi t^2} \right)^{\frac{q-1}{q}} & \text{if } q \in [1, \infty), \\[4mm] \dfrac{\sqrt{3}}{2\pi t^2} & \text{if } q = \infty. \end{cases} \qquad (t > 0).$$

Combining the above estimates with Young's inequality, we obtain

Corollary 2.1. *Let* $p, q, r \in [1, \infty]$ *such that* $\frac{1}{p} + \frac{1}{q} = 1 + \frac{1}{r}$*.*

If $f_0 \in L^p(\mathbb{R}^2)$*, then the solution* f *of* (1) *satisfies for every* $t > 0$*,* $f(t) \in L^r(\mathbb{R}^2)$ *and*

$$\|f(t)\|_{L^r(\mathbb{R}^2)} \leqslant \begin{cases} \dfrac{C(q)}{t^{2(1-\frac{1}{q})}} \|f_0\|_{L^p(\mathbb{R}^2)} & \text{if } q \in [1, \infty), \\[4mm] \dfrac{C(q)}{t^2} \|f_0\|_{L^p(\mathbb{R}^2)} & \text{if } q = \infty, \end{cases}$$

with $C(q) = q^{\frac{-1}{q}} \left(\frac{\sqrt{3}}{2\pi} \right)^{\frac{q-1}{q}}$ if $q \in [1, \infty)$ and $C(q) = \frac{\sqrt{3}}{2\pi}$ if $q = \infty$.

Remark 2.1. Since $g(t, \cdot, \cdot)$ is obtained by the change of variable (2), we have $\|g(t)\|_{L^r(\mathbb{R}^2)} = \|f(t)\|_{L^r(\mathbb{R}^2)}$ and consequently, it is expected that the decay rate in time of g is also polynomial.

3. Self-similar formulation of the Kolmogorov operator

In this section we derive the self-similar form eq. (5) for the Kolmogorov Equation (1). In addition, we prove the convergence of $\widetilde{f}$, the solution to eq. (5), to a steady state as time tends to infinity. Moreover, we give a remark establishing that the behavior of the norm of $\widetilde{f}$ is not monotonic.

Let us introduce the function g from eq. (2) to obtain eq. (3). Now define the change of variables

$$\begin{cases} t = e^s - 1, \\ v = e^{s/2}\widetilde{v}, \qquad ((s, \widetilde{v}, \widetilde{x}) \in \mathbb{R}_+ \times \mathbb{R} \times \mathbb{R}) \\ z = e^{3s/2}\widetilde{x} \end{cases}$$

and define:

$$\widetilde{f}(s, \widetilde{v}, \widetilde{x}) = e^{2s} g(t, v, z).$$

Then, $\widetilde{f}$ is the solution to the initial value problem

$$\partial_s \widetilde{f} = \partial_{\widetilde{v}}^2 \widetilde{f} + 2(1 - e^{-s}) \partial_{\widetilde{v}\widetilde{x}} \widetilde{f} + (1 - e^{-s})^2 \partial_{\widetilde{x}\widetilde{x}} \widetilde{f} + \frac{1}{2} \widetilde{v} \partial_{\widetilde{v}} \widetilde{f} + \frac{3}{2} \widetilde{x} \partial_{\widetilde{x}} \widetilde{f} + 2 \widetilde{f},$$

$$\widetilde{f}(0, \cdot, \cdot) = f_0.$$

(5)

Since eq. (5) is obtained from eq. (1) by a change of variables, it is straightforward to show that this equation admits a unique solution.

Let us now give some qualitative behavior of $\widetilde{f}$. More precisely, we discuss the behavior of the norm of $\widetilde{f}$. It is easy to see that

$$\frac{1}{2} \frac{d}{ds} \|\widetilde{f}(s)\|_{L^2(\mathbb{R}^2)}^2 = - \left\| (1 - e^{-s}) \partial_{\widetilde{x}} \widetilde{f}(s) + \partial_{\widetilde{v}} \widetilde{f}(s) \right\|_{L^2(\mathbb{R}^2)}^2 + \left\| \widetilde{f}(s) \right\|_{L^2(\mathbb{R}^2)}^2 \qquad (s > 0).$$

So we see the evolution of the norm of $\widetilde{f}$ is the result of competition between the norm of $\widetilde{f}$ and the norm of the "divergence" of $\widetilde{f}$. But since we are working on an unbounded domain, we cannot use a Poincaré inequality to give a precise result on the behavior of the norm of $\widetilde{f}$.

However, using the integral representation of g, we can give a more precise statement for the behavior of the L^∞ norm of g.

Proposition 3.1. Let us assume that $f_0 \in L^1(\mathbb{R}^2) \cap L^\infty(\mathbb{R}^2)$, then the solution $\widetilde{f}$ of eq. (5) satisfies

$$\|\widetilde{f}(s, \cdot, \cdot)\|_{L^\infty(\mathbb{R}^2)} \leqslant \min \left\{ \frac{\sqrt{3}}{2\pi} \frac{1}{(1 - e^{-s})^2} \|f_0\|_{L^1(\mathbb{R}^2)}, \; e^{2s} \|f_0\|_{L^\infty(\mathbb{R}^2)} \right\} \qquad (s > 0).$$

Remark 3.1. It is easy to see that we also have

$$\|\widetilde{f}(s, \cdot, \cdot)\|_{L^\infty(\mathbb{R}^2)} \leqslant C(s) \max \left\{ \|f_0\|_{L^1(\mathbb{R}^2)}, \; \|f_0\|_{L^\infty(\mathbb{R}^2)} \right\} \qquad (s > 0),$$

with $C(s) = \min \left\{ \frac{\sqrt{3}}{2\pi} \frac{1}{(1 - e^{-s})^2}, \; e^{2s} \right\}$. The behavior of C is plotted on Fig. 1.

Proof. Recall:

$$\widetilde{f}(s, \widetilde{v}, \widetilde{x}) = e^{2s} g(e^s - 1, e^{s/2}\widetilde{v}, e^{3s/2}\widetilde{x}) \qquad ((s, \widetilde{v}, \widetilde{x}) \in \mathbb{R} \times \mathbb{R} \times \mathbb{R})$$

and hence, for $(s, \widetilde{v}, \widetilde{x}) \in \mathbb{R} \times \mathbb{R} \times \mathbb{R}$,

$$\widetilde{f}(s, \widetilde{v}, \widetilde{x}) = e^{2s} \int_{\mathbb{R}^2} G_{e^s - 1}(v, \zeta) f_0(e^{s/2}\widetilde{v} - v, e^{3/2s}\widetilde{x} - \zeta) \, dv d\zeta$$

$$= e^{4s} \int_{\mathbb{R}^2} G_{e^s - 1}(e^{s/2}\widetilde{v}, e^{3s/2}\widetilde{\zeta}) f_0(e^{s/2}(\widetilde{v} - \widetilde{v}), e^{3/2s}(\widetilde{x} - \widetilde{\zeta})) \, d\widetilde{v} d\widetilde{\zeta}.$$
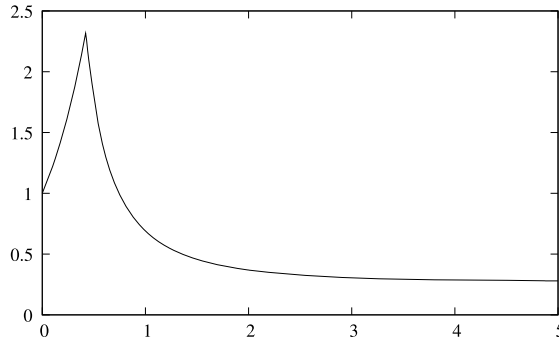
Fig. 1. Graphical representation of $s \mapsto \min\left\{\frac{\sqrt{3}}{2\pi}\frac{1}{(1-e^{-s})^2}, e^{2s}\right\}$.

Hence, using Young's inequality, for every $s > 0$, we have

$$\|\widetilde{f}(s)\|_{L^\infty(\mathbb{R}^2)} \leqslant e^{2s}\left\|G_{e^s-1}(e^{s/2}\cdot, e^{3s/2}\cdot)\right\|_{L^\infty(\mathbb{R}^2)}\left\|e^{2s}f_0(e^{s/2}\cdot, e^{3/2s}\cdot)\right\|_{L^1(\mathbb{R}^2)}.$$

Consequently, using Lemma 2.1,

$$\|\widetilde{f}(s)\|_{L^\infty(\mathbb{R}^2)} \leqslant \frac{\sqrt{3}}{2\pi}\frac{1}{(1-e^{-s})^2}\|f_0\|_{L^1(\mathbb{R}^2)}.$$

On the other hand, since $f_0 \in L^\infty(\mathbb{R}^2)$, applying again Young's inequality, we also obtain:

$$\|\widetilde{f}(s)\|_{L^\infty(\mathbb{R}^2)} \leqslant e^{2s}\|G_{e^s-1}\|_{L^1(\mathbb{R}^2)}\|f_0\|_{L^\infty(\mathbb{R}^2)} \qquad (s > 0)$$

and Lemma 2.1, gives:

$$\|\widetilde{f}(s)\|_{L^\infty(\mathbb{R}^2)} \leqslant e^{2s}\|f_0\|_{L^\infty(\mathbb{R}^2)} \qquad (s > 0). \quad \square$$

Let us now consider the asymptotic behavior of the norm of the solution to eq. (5), $\widetilde{f}$, as $s \to \infty$.

Theorem 3.1 (*Long time behavior of $\widetilde{f}$*). *Let $p \in [1, \infty]$ and $f_0 \in L^1(\mathbb{R}^2) \cap L^p(\mathbb{R}^2)$. If $p = \infty$, we assume in addition, $f_0 \in C^0(\mathbb{R}^2)$.*
Set $M_0 = \displaystyle\int_{\mathbb{R}^2} f_0(v, x)\,\mathrm{d}v\,\mathrm{d}x$ and assume $M_0 \neq 0$.
Then the solution $\widetilde{f}$ of eq. (5) with initial Cauchy data f_0 satisfies:

$$\lim_{s\to\infty}\|\widetilde{f}(s, \cdot, \cdot) - M_0 G_1\|_{L^p(\mathbb{R}^2)} = 0.$$

Proof. Let us first assume that $f_0 \in C_c^\infty(\mathbb{R}^2)$. The solution of eq. (3) with initial Cauchy data f_0 is given by:

$$g(t, v, z) = (G_t * f_0)(v, z) = \int_{\mathbb{R}^2} G_t(v, \zeta)f_0(v - \nu, z - \zeta)\,\mathrm{d}\nu\,\mathrm{d}\zeta \qquad ((t, v, z) \in \mathbb{R}_+ \times \mathbb{R} \times \mathbb{R}),$$

with G given by eq. (4). Hence, in terms of self-similar variables, we have, as in the proof of Proposition 3.1,

$$\widetilde{f}(s, \widetilde{v}, \widetilde{x}) = e^{4s}\int_{\mathbb{R}^2} G_{e^s-1}(e^{s/2}\widetilde{v}, e^{3s/2}\widetilde{\zeta})\,f_0(e^{s/2}(\widetilde{v} - \widetilde{\nu}), e^{3/2s}(\widetilde{x} - \widetilde{\zeta}))\,\mathrm{d}\widetilde{\nu}\,\mathrm{d}\widetilde{\zeta} \qquad ((s, \widetilde{v}, \widetilde{x}) \in \mathbb{R}_+ \times \mathbb{R} \times \mathbb{R}).$$

But, we have from eq. (4),

$$e^{2s}G_{e^s-1}\left(e^{s/2}\widetilde{v}, e^{3s/2}\widetilde{\zeta}\right)$$

$$= \frac{e^{2s}\sqrt{3}}{2\pi(e^s-1)^2}\exp\left(\frac{-\left(3e^{3s}\widetilde{\zeta}^2 + \left(2(e^s-1)e^{s/2}\widetilde{v} - 3e^{3s/2}\widetilde{\zeta}\right)^2\right)}{4(e^s-1)^3}\right)$$

$$= \frac{\sqrt{3}}{2\pi(1-e^{-s})^2}\exp\left(\frac{-\left(3\widetilde{\zeta}^2 + \left(2(1-e^{-s})\widetilde{v} - 3\widetilde{\zeta}\right)^2\right)}{4(1-e^{-s})^3}\right)$$

$$= G_{1-e^{-s}}\left(\widetilde{v}, \widetilde{\zeta}\right).$$

Thus,

$$\widetilde{f}(s,\widetilde{v},\widetilde{x}) = \left(G_{1-e^{-s}} * \gamma_s\right)(\widetilde{v},\widetilde{x}) = (G_1 * \gamma_s)(\widetilde{v},\widetilde{x}) + \left((G_{1-e^{-s}} - G_1) * \gamma_s\right)(\widetilde{v},\widetilde{x}),$$

where we have set, $\gamma_s(\widetilde{v},\widetilde{x}) = e^{2s} f_0\left(e^{s/2}\widetilde{v}, e^{3/2s}\widetilde{x}\right)$.

Let us notice that,

$$\int_{\mathbb{R}^2} M_0^{-1} \gamma_s(\widetilde{v},\widetilde{x})\, d\widetilde{v}d\widetilde{x} = M_0^{-1} \int_{\mathbb{R}^2} f_0(v,x)\, dv dx = 1 \quad \text{and} \quad \left\|M_0^{-1}\gamma_s\right\|_{L^1(\mathbb{R}^2)} = \left|M_0^{-1}\right| \|f_0\|_{L^1(\mathbb{R}^2)} < \infty \qquad (s \geqslant 0)$$

and, since f_0 has a compact support, for every $\varepsilon > 0$, there exists $s_0 \geqslant 0$ large enough such that for every $s \geqslant s_0$, we have supp $\gamma_s \subset B(\varepsilon)$ (with $B(\varepsilon)$ the ball of $\mathbb{R}^2$ of radius ε centered at 0).

Consequently, $(M_0^{-1}\gamma_s)_{s \geqslant 0}$ is an approximate identity sequence, and hence, for every $p \in [1,\infty]$, we have,

$$\lim_{s\to\infty} \|G_1 * \gamma_s - M_0 G_1\|_{L^p(\mathbb{R}^2)} = 0.$$

In order to finish the proof, it remains to prove that

$$\lim_{s\to\infty} \left\|(G_{1-e^{-s}} - G_1) * \gamma_s\right\|_{L^p(\mathbb{R}^2)} = 0.$$

But Young's inequality ensures that

$$\left\|(G_{1-e^{-s}} - G_1) * \gamma_s\right\|_{L^p(\mathbb{R}^2)} \leqslant \|\gamma_s\|_{L^1(\mathbb{R}^2)} \left\|G_{1-e^{-s}} - G_1\right\|_{L^p(\mathbb{R}^2)} \qquad (s \geqslant 0),$$

that is to say, for every $s \geqslant 0$,

$$\left\|(G_{1-e^{-s}} - G_1) * \gamma_s\right\|_{L^p(\mathbb{R}^2)} \leqslant M_0^{-1} \|f_0\|_{L^1(\mathbb{R}^2)} \left\|G_{1-e^{-s}} - G_1\right\|_{L^p(\mathbb{R}^2)}.$$

Consequently, in the rest of this proof we will prove that

$$\lim_{\sigma\to 0} \|G_{1-\sigma} - G_1\|_{L^p(\mathbb{R}^2)} = 0.$$

For every $(\sigma, v, \zeta) \in [0,1) \times \mathbb{R} \times \mathbb{R}$, we have

$$
\begin{aligned}
G_{1-\sigma}(v,\zeta) &= \frac{\sqrt{3}}{2\pi(1-\sigma)^2} \exp\left(\frac{-1}{(1-\sigma)^3}\left(3\zeta^2 - 3(1-\sigma)\zeta v + (1-\sigma)^2 v^2\right)\right) \\
&= \frac{\sqrt{3}}{2\pi}\left(\frac{1}{(1-\sigma)^2} - 1\right) \exp\left(\frac{-1}{(1-\sigma)^3}\left(3\zeta^2 - 3(1-\sigma)\zeta v + (1-\sigma)^2 v^2\right)\right) \\
&\quad + \frac{\sqrt{3}}{2\pi} \exp\left(\frac{-1}{(1-\sigma)^3}\left(3\zeta^2 - 3(1-\sigma)\zeta v + (1-\sigma)^2 v^2\right)\right) \\
&= \sigma(2-\sigma)G_{1-\sigma}(v,\zeta) \\
&\quad + \exp\left(\frac{-1}{(1-\sigma)^3}\left(3\zeta^2 - 3(1-\sigma)\zeta v + (1-\sigma)^2 v^2\right) + \left(3\zeta^2 - 3\zeta v + v^2\right)\right)G_1(v,\zeta) \\
&= \sigma(2-\sigma)G_{1-\sigma}(v,\zeta) \\
&\quad + \exp\left(\frac{-\sigma}{(1-\sigma)^3}\left(3\left(3 - 3\sigma + \sigma^2\right)\zeta^2 - 3(1-\sigma)(2-\sigma)\zeta v + (1-\sigma)^2 v^2\right)\right)G_1(v,\zeta) \\
&= \sigma(2-\sigma)G_{1-\sigma}(v,\zeta) + \varphi_\sigma(v,\zeta)G_1(v,\zeta),
\end{aligned}
$$

with $\varphi_\sigma(v,\zeta) = \exp\left(-(\zeta, v)A_\sigma(\zeta, v)^\top\right)$, where we have defined

$$A_\sigma = \frac{\sigma}{(1-\sigma)^3}\begin{pmatrix} 3\left(3 - 3\sigma + \sigma^2\right) & \frac{3}{2}(1-\sigma)(2-\sigma) \\ \frac{3}{2}(1-\sigma)(2-\sigma) & (1-\sigma)^2 \end{pmatrix}.$$

Consequently, we have

$$
\begin{aligned}
G_{1-\sigma}(v,\zeta) - G_1(v,\zeta) &= \frac{\varphi_\sigma(v,\zeta)}{1-\sigma(2-\sigma)}G_1(v,\zeta) - G_1(v,\zeta) \\
&= \frac{1}{1-\sigma(2-\sigma)}(\varphi_\sigma(v,\zeta)G_1(v,\zeta) - G_1(v,\zeta)) - \frac{\sigma(2-\sigma)}{1-\sigma(2-\sigma)}G_1(v,\zeta)
\end{aligned}
$$

and so

$$\|G_{1-\sigma} - G_1\|_{L^p(\mathbb{R}^2)} \leqslant \frac{1}{|1 - \sigma(2-\sigma)|} \|(\varphi_\sigma - 1)G_1\|_{L^p(\mathbb{R}^2)} + \left|\frac{\sigma(2-\sigma)}{1 - \sigma(2-\sigma)}\right| \|G_1\|_{L^p(\mathbb{R}^2)}.$$

It is clear that $\lim\limits_{\sigma \to 0} \left|\frac{\sigma(2-\sigma)}{1 - \sigma(2-\sigma)}\right| \|G_1\|_{L^p(\mathbb{R}^2)} = 0$. Thus, it remains to prove that $\lim\limits_{\sigma \to 0} \|(\varphi_\sigma - 1)G_1\|_{L^p(\mathbb{R}^2)} = 0$.

One can easily compute that $\det A_\sigma > 0$ and $\operatorname{Tr} A_\sigma > 0$ for every $\sigma \in (0,1]$. This ensures that for every $\sigma \in (0,1)$, φ_σ is bounded by 1 on $\mathbb{R}^2$ and exponentially decays to 0 at infinity. In addition, the eigenvalues of A_σ are of order σ as $\sigma \to 0$.

Let us denote λ_σ the largest eigenvalue of A_σ. Then for every $R \in \mathbb{R}_+^*$, every $\sigma \in (0,1)$ and every $p \in [1, \infty]$, we have:

$$\begin{aligned}
\|\varphi_\sigma G_1 - G_1\|_{L^p(\mathbb{R}^2)} &= \|(\varphi_\sigma - 1)G_1\|_{L^p(B(R))} + \|(\varphi_\sigma - 1)G_1\|_{L^p(\mathbb{R}^2 \setminus B(R))} \\
&\leqslant \|\varphi_\sigma - 1\|_{L^\infty(B(R))} \|G_1\|_{L^p(B(R))} + \|(\varphi_\sigma - 1)G_1\|_{L^p(\mathbb{R}^2 \setminus B(R))} \\
&\leqslant \left(1 - e^{-\lambda_\sigma R}\right) \|G_1\|_{L^p(\mathbb{R}^2)} + \|G_1\|_{L^p(\mathbb{R}^2 \setminus B(R))},
\end{aligned}$$

where $B(R) \subset \mathbb{R}^2$ is the ball of radius R centered at 0. Consequently, since $\lim\limits_{\sigma \to 0} \lambda_\sigma = 0$ and G_1 decays exponentially to 0 at infinity, by taking $R = R_\sigma = \frac{1}{\sqrt{\lambda_\sigma}}$, it follows that $\lim\limits_{\sigma \to 0}\left(1 - e^{-\lambda_\sigma R_\sigma}\right) = 0$ and $\lim\limits_{\sigma \to 0} \|G_1\|_{L^p(\mathbb{R}^2 \setminus B(R_\sigma))} = 0$. That is to say, $\lim\limits_{\sigma \to 0} \|(\varphi_\sigma - 1)G_1\|_{L^p(\mathbb{R}^2)} = 0$.

All in all,

$$\lim_{s \to \infty} \|\widetilde{f}(s, \cdot, \cdot) - M_0 G_1\|_{L^p(\mathbb{R}^2)} = 0 \qquad (p \in [1, \infty])$$

and the result follows from density arguments. □

4. Restriction to a bounded domain

Since the numerical simulations will be performed in a truncated domain, let us first start this section with some results on the behavior of the solution to eqs. (1), (3) and (5) in a bounded domain with homogeneous Dirichlet boundary conditions. In addition, in the self-similar formulation, we will also present a convergence result for the *truncated* solution to the *full* solution as the size of the domain goes to infinity.

In this section we aim to study the impact of changing the space domain $\mathbb{R}^2$ to a bounded domain $\Omega \subset \mathbb{R}^2$ with homogeneous Dirichlet boundary conditions. First, let us remind the reader that according to Corollary 2.1, the decay in L^2-norm of the solution, f, set in the whole space $\mathbb{R}^2$ is polynomial. In § 4.1 we will see that the solution of the equation in the original form (1) converges exponentially to 0, when we truncate the space domain to a bounded domain. In § 4.3, existence and uniqueness of a solution to the truncated self-similar equation and convergence of the bounded domain problem to the full space problem are proven in Proposition 4.1 and Proposition 4.2. A condition such that the truncated solution does not tend to 0 as time goes to infinity is given in Proposition 4.3.

The results presented here are consequences of the following Poincaré inequality.

Lemma 4.1. *Let $\Omega \subset \mathbb{R}^2$ be a bounded domain and set I_v and I_x be two open and bounded intervals of $\mathbb{R}$ such that $\Omega \subset I_v \times I_x$. Then for every $\big((v,x) \mapsto g(v,x)\big) \in H_0^1(\Omega)$ and every $t \geqslant 0$, there exists $C_\Omega(t) \in \mathbb{R}_+^*$ such that:*

$$\|g\|_{L^2(\Omega)}^2 \leqslant C_\Omega(t) \|\partial_v g + t \partial_x g\|_{L^2(\Omega)}^2,$$

with,

$$C_\Omega(t) \leqslant C_{I_v \times I_x}(t) \leqslant \begin{cases} \dfrac{|I_v|^2}{2} & \text{if } 0 \leqslant \dfrac{|I_v|}{|I_x|} t \leqslant 1, \\[3mm] \dfrac{|I_x|^2}{2t^2} & \text{if } 1 \leqslant \dfrac{|I_v|}{|I_x|} t. \end{cases} \tag{6}$$

The proof of this result is given in Appendix A.

4.1. The Kolmogorov equation

In this subsection we show that the asymptotic behavior of (1) simulated on a truncated domain with Dirichlet boundary conditions is no longer polynomial and is, in fact, exponential.

To this end, let us consider (1) on a bounded domain Ω, i.e.

$$\partial_t f = v \partial_x f + \partial_v^2 f \qquad \text{in } \mathbb{R}_+^* \times \Omega,$$
$$f = 0 \qquad \text{on } \mathbb{R}_+^* \times \partial\Omega,$$
$$f = f_0 \qquad \text{on } \{0\} \times \Omega.$$

It is easy to see that

$$\frac{1}{2}\frac{d}{dt}\|f(t)\|_{L^2(\Omega)}^2 = -\|\partial_v f(t)\|_{L^2(\Omega)}^2 \qquad (t > 0).$$

Now using Lemma 4.1 for $t = 0$, it follows that

$$\frac{d}{dt}\|f(t)\|_{L^2(\Omega)}^2 \leqslant -2C_\Omega(0)^{-1}\|f(t)\|_{L^2(\Omega)}^2,$$

with $C_\Omega(0) > 0$ defined in Lemma 4.1. Thus, using Grönwall's lemma, we obtain:

$$\|f(t)\|_{L^2(\Omega)} \leqslant \|f_0\|_{L^2(\Omega)} \exp\frac{-t}{C_\Omega(0)} \qquad (t \geqslant 0).$$

Consequently, this direct simulation cannot be used in order to capture the long time behavior of the solution, since the expected decay rate is polynomial.

4.2. The rotating form

As in § 4.1, we show in this subsection that the asymptotic of (2) simulated on a truncated domain with Dirichlet boundary conditions is no longer polynomial and is, in fact, exponential.

To this end, let us consider (3) on a bounded domain Ω, i.e.

$$\partial_t g = \partial_v^2 g + 2t \partial_v \partial_x g + t^2 \partial_x^2 g \qquad \text{in } \mathbb{R}_+^* \times \Omega,$$
$$g = 0 \qquad \text{on } \mathbb{R}_+^* \times \partial\Omega,$$
$$g = f_0 \qquad \text{on } \{0\} \times \Omega.$$

It is easy to see that

$$\frac{1}{2}\frac{d}{dt}\|g(t)\|_{L^2(\Omega)}^2 = -\|\partial_v f(t) + t \partial_x g\|_{L^2(\Omega)}^2 \qquad (t > 0).$$

Now using Lemma 4.1 for $t \geqslant 0$, it follows that

$$\frac{d}{dt}\|g(t)\|_{L^2(\Omega)}^2 \leqslant -2C_\Omega(t)^{-1}\|g(t)\|_{L^2(\Omega)}^2,$$

with $C_\Omega(t) > 0$ defined in Lemma 4.1. Thus, using Grönwall's lemma, we obtain:

$$\|g(t)\|_{L^2(\Omega)} \leqslant \|f_0\|_{L^2(\Omega)} \exp\int_0^t \frac{-ds}{C_\Omega(s)} \qquad (t \geqslant 0).$$

Let I_v and I_x be two open and bounded intervals of $\mathbb{R}$ such that $\Omega \subset I_v \times I_x$ then from the estimate (6), we have,

$$\int_0^t \frac{ds}{C_\Omega(s)} \geqslant \begin{cases} \frac{2t}{|I_v|^2} & \text{if } t \leqslant \frac{|I_x|}{|I_v|}, \\ \frac{4|I_x|}{3|I_v|^3} + \frac{2t^3}{3|I_x|^2} & \text{if } t > \frac{|I_x|}{|I_v|}. \end{cases}$$

Consequently, we have $\leqslant \|g(t)\|_{L^2(\Omega)} = O_{t\to\infty}\left(e^{\frac{2t^3}{3|I_x|^2}}\right)$. Consequently, this direct simulation cannot be used in order to capture the long time behavior of the solution, since the expected decay rate is polynomial, see Remark 2.1.

4.3. The self-similar form

Now in contrast to the results in the previous subsection, we will show in this subsection that using a self-similar change of variables allows one to simulate (1) on a truncated domain with Dirichlet boundary conditions and still preserve the polynomial decay. Thus, a self-similar change of variables is indeed a useful method for preserving asymptotic decay rates.

Let us consider the self-similar form of (1), i.e. (5), on a bounded domain, Ω,

$$\partial_s \widetilde{f} = \partial_{\widetilde{v}}^2 \widetilde{f} + 2(1 - e^{-s})\partial_{\widetilde{v}}\partial_{\widetilde{x}}\widetilde{f} + (1 - e^{-s})^2\partial_{\widetilde{x}}^2\widetilde{f} + \tfrac{1}{2}\widetilde{v}\partial_{\widetilde{v}}\widetilde{f} + \tfrac{3}{2}\widetilde{x}\partial_{\widetilde{x}}\widetilde{f} + 2\widetilde{f} \qquad \text{in } \mathbb{R}_+^* \times \Omega, \tag{7a}$$

$$\widetilde{f} = 0 \qquad\qquad\qquad\qquad \text{on } \mathbb{R}_+^* \times \partial\Omega, \tag{7b}$$

$$\widetilde{f} = f_0 \qquad\qquad\qquad\qquad \text{on } \{0\} \times \Omega. \tag{7c}$$

In Proposition 4.1 we prove that (7) admits a unique solution. Then, in Proposition 4.2 we show that if the truncated domain is converging to the full space, then the *truncated solution* is also converging to the *full* one i.e. to the solution of (5).

Proposition 4.1. *Let $f_0 \in L^2(\Omega)$, then there exists a unique solution $\widetilde{f} \in C^1([0, T], L^2(\Omega))$ for* (7).
Moreover, we have

$$\|\widetilde{f}(s)\|_{L^2(\Omega)} \leqslant \exp\left(s - \int_0^s \frac{\mathrm{d}\sigma}{C_\Omega(1 - e^{-\sigma})}\right)\|f_0\|_{L^2(\Omega)} \qquad (s \geqslant 0), \tag{8}$$

with $C_\Omega(\cdot)$ defined in Lemma 4.1.

Proof. In order to prove that (7) has a unique solution, we consider the following equivalent form of (7).
Define $\mathfrak{f} = \widetilde{f}e^{-2s}$, then $\mathfrak{f}$ satisfies the following equation

$$\partial_s\mathfrak{f} = -\mathcal{F}(\mathfrak{f}) := \partial_{\widetilde{v}}^2\mathfrak{f} + 2(1 - e^{-s})\partial_{\widetilde{v}}\partial_{\widetilde{x}}\mathfrak{f} + (1 - e^{-s})^2\partial_{\widetilde{x}}^2\mathfrak{f} + \tfrac{1}{2}\widetilde{v}\partial_{\widetilde{v}}\mathfrak{f} + \tfrac{3}{2}\widetilde{x}\partial_{\widetilde{x}}\mathfrak{f} \qquad \text{in } \mathbb{R}_+^* \times \Omega, \tag{9a}$$

$$\mathfrak{f} = 0 \qquad\qquad\qquad\qquad \text{on } \mathbb{R}_+^* \times \partial\Omega, \tag{9b}$$

$$\mathfrak{f} = f_0 \qquad\qquad\qquad\qquad \text{on } \{0\} \times \Omega. \tag{9c}$$

A classical argument shows that $\mathcal{F}$ is a continuous operator in $L^2(\Omega)$. We show that $\mathcal{F}$ is also coercive

$$\int_\Omega \mathcal{F}(\mathfrak{f})\mathfrak{f}\mathrm{d}\widetilde{v}\mathrm{d}\widetilde{x} = \int_\Omega \left|\partial_{\widetilde{v}}\mathfrak{f} + (1 - e^{-s})\partial_{\widetilde{x}}\mathfrak{f}\right|^2 \mathrm{d}\widetilde{v}\mathrm{d}\widetilde{x} + \int_\Omega |\mathfrak{f}|^2 \mathrm{d}\widetilde{v}\mathrm{d}\widetilde{x}. \tag{10}$$

The existence and uniqueness of a solution to (9) then follows and estimate (8) follows from (10), Lemma 4.1 and Grönwall's lemma. $\square$

For every $\varphi \in \mathcal{D}(\mathbb{R}_+ \times \mathbb{R}^2)'$, a distribution on $\mathbb{R}_+ \times \mathbb{R}^2$, we define

$$K\varphi = \partial_s\varphi - \left(\partial_{\widetilde{v}} + (1 - e^{-s})\partial_{\widetilde{x}}\right)^2\varphi - \left(\frac{1}{2}\widetilde{v}\partial_{\widetilde{v}} + \frac{3}{2}\partial_{\widetilde{x}}\right)\varphi - 2\varphi \qquad \text{and}$$

$$K^*\varphi = -\partial_s\varphi - \left(\partial_{\widetilde{v}} + (1 - e^{-s})\partial_{\widetilde{x}}\right)^2\varphi + \left(\frac{1}{2}\widetilde{v}\partial_{\widetilde{v}} + \frac{3}{2}\partial_{\widetilde{x}}\right)\varphi.$$

Proposition 4.2. *Consider the sequence of bounded domains of $\mathbb{R}^2$, $\{\Omega_N\}_{N\in\mathbb{N}^*}$ and assume:*

$$\bigcup_{N\in\mathbb{N}^*} \Omega_N = \mathbb{R}^2 \quad and \quad \Omega_1 \subset \Omega_2 \subset \cdots \subset \Omega_N \subset \cdots \subset \mathbb{R}^2.$$

Set $f_0 \in C_c(\mathbb{R}^2)$. Then the equation

$$\partial_s g_N = \partial_{\widetilde{v}}^2 g_N + 2(1 - e^{-s})\partial_{\widetilde{v}}\partial_{\widetilde{x}}g_N + (1 - e^{-s})^2\partial_{\widetilde{x}}^2 g_N + \tfrac{1}{2}\widetilde{v}\partial_{\widetilde{v}}g_N + \tfrac{3}{2}\widetilde{x}\partial_{\widetilde{x}}g_N + 2g_N \qquad \text{in } \mathbb{R}_+^* \times \Omega_N, \tag{11a}$$

$$g_N = 0 \qquad\qquad\qquad\qquad \text{on } \mathbb{R}_+^* \times \partial\Omega_N, \tag{11b}$$

$$g_N = f_0|_{\Omega_N} \qquad\qquad\qquad\qquad \text{on } \{0\} \times \Omega_N, \tag{11c}$$

has a unique solution g_N in $C^1([0, T], L^2(\Omega_N))$.
Moreover, for every $T > 0$, then, there exists a subsequence of $(g_N)_N$ which converges in the weak topology of $L^2([0, T] \times \mathbb{R}^2)$ to the solution g_* of (7) *in the following sense*

$$0 = \int_{\mathbb{R}^2} \varphi(0, \cdot)f_0 + \int_{[0,T]\times\mathbb{R}^2} g_* K^*\varphi,$$

for every $\varphi \in C_c^\infty([0, T) \times \mathbb{R}^2)$. In addition, all convergent subsequences of $(g_N)_N$ are weakly convergent in $L^2((0, T) \times \mathbb{R}^2)$ to a solution of (7) *in the sense mentioned above.*

Proof. The existence and uniqueness of g_N is provided by Proposition 4.1.

Let us classically extend g_N by 0 outside Ω_N. We now prove the weak convergence of $(g_N)_N$ to $\widetilde{f}$. Thus, according to (8), for every $N \in \mathbb{N}^*$ we have

$$\|g_N(s)\|_{L^2(\mathbb{R}^2)} = \|g_N(s)\|_{L^2(\Omega_N)} \leqslant \exp\left(s - \int_0^s \frac{d\sigma}{C_{\Omega_N}(1 - e^{-\sigma})}\right) \|f_0\|_{L^2(\Omega_N)} \leqslant e^s \|f_0\|_{L^2(\mathbb{R}^2)} \qquad (s \in [0, T]) .$$

This ensures that up to a subsequence the sequence $(g_N)_N$ is convergent to some $g_* \in L^2([0, T] \times \mathbb{R}^2)$ for the weak topology of $L^2([0, T] \times \mathbb{R}^2)$. Let us still denote by $(g_N)_N$ this convergent subsequence. Now, for every $\varphi \in C_c^\infty([0, T) \times \mathbb{R}^2)$, there exists $N_0 \in \mathbb{N}^*$ such that for every $N \geqslant N_0$, we have $\operatorname{supp} \varphi \subset [0, T) \times \Omega_N$. Since g_N is solution of (11), we have, $0 = \int_{[0,T] \times \mathbb{R}^2} \varphi K g_N$ and integrating by parts, we obtain,

$$0 = \int_{\mathbb{R}^2} \varphi(0, \cdot) f_0 + \int_{[0,T] \times \mathbb{R}^2} g_N K^* \varphi .$$

But, since $\varphi \in C_c^\infty([0, T) \times \mathbb{R}^2)$, we have $K^* \varphi \in L^2([0, T] \times \mathbb{R}^2)$ and by the weak convergence of $(g_N)_N$, we have, taking the limit $N \to \infty$,

$$0 = \int_{\mathbb{R}^2} \varphi(0, \cdot) f_0 + \int_{[0,T] \times \mathbb{R}^2} g_* K^* \varphi ,$$

for all $\varphi \in C_c^\infty([0, T) \times \mathbb{R}^2)$. $\square$

While the self-similarity change of variables can indeed provide a method for preserving the polynomial decay of solutions, this method is very reliant on the following condition to be able to provide for such decay rates.

Proposition 4.3. *Given $\widetilde{f}$ the solution to (7) and let $\Omega \subset \mathbb{R}^2$ be a bounded domain and let I_v and I_x be two bounded intervals of $\mathbb{R}$ such that $\Omega \subset I_v \times I_x \subset \mathbb{R}^2$.*

In order to avoid the exponential convergence of $\widetilde{f}$ to zero as $t \to \infty$, I_v and I_x shall satisfy

$$|I_v| \geqslant \sqrt{2} \qquad and \qquad |I_x| \geqslant \sqrt{2} . \tag{12}$$

Proof. Using (8) together with the estimates (6), we have

$$\|\widetilde{f}(s)\|_{L^2(\Omega)} \leqslant \exp\left(s - \int_0^s \frac{d\sigma}{\widetilde{C}(1 - e^{-\sigma})}\right) \|f_0\|_{L^2(\Omega)} \qquad (s \geqslant 0) ,$$

with

$$\widetilde{C}(t) = \begin{cases} \dfrac{|I_v|^2}{2} & \text{if } 0 \leqslant \dfrac{|I_v|}{|I_x|} t \leqslant 1 , \\[4mm] \dfrac{|I_x|^2}{2t^2} & \text{if } 1 \leqslant \dfrac{|I_v|}{|I_x|} t . \end{cases} \qquad (t \geqslant 0) .$$

But,

1. if $|I_v| \leqslant |I_x|$, then $\widetilde{C}(1 - e^{-\sigma}) = \frac{|I_v|^2}{2}$ for every $\sigma \geqslant 0$. Thus,

$$\int_0^s \frac{d\sigma}{\widetilde{C}(1 - e^{-\sigma})} = \frac{2s}{|I_v|^2} \qquad (s \geqslant 0) ;$$

2. if $|I_v| > |I_x|$,

let us define $s_0 = \ln \frac{|I_v|}{|I_v| - |I_x|}$, i.e. $\frac{|I_v|}{|I_x|}(1 - e^{-s_0}) = 1$, then,

$$\widetilde{C}(1 - e^{-\sigma}) = \begin{cases} \dfrac{|I_v|^2}{2} & \text{if } \sigma \leqslant s_0 , \\[4mm] \dfrac{|I_x|^2}{2(1 - e^{-\sigma})^2} & \text{if } \sigma > s_0 \end{cases}$$

and consequently, if $s \leqslant s_0$ we have

$$\int_0^s \frac{d\sigma}{\widetilde{C}(1 - e^{-\sigma})} = \frac{2s}{|I_v|^2}$$

and if $s > s_0$ we have

$$\int_0^s \frac{d\sigma}{\widetilde{C}(1 - e^{-\sigma})} = \frac{2s_0}{|I_v|^2} + \frac{2}{|I_x|^2} \int_{s_0}^s (1 - e^{-\sigma})^2 \, d\sigma$$

$$= \frac{2s_0}{|I_v|^2} + \frac{2}{|I_x|^2} \left(s - s_0 + 2e^{-s} - 2e^{-s_0} - \frac{1}{2}e^{-2s} + \frac{1}{2}e^{-2s_0} \right) = \frac{2s}{|I_x|^2} + O_{s \to \infty}(1) .$$

According to Theorem 3.1 it is expected that the solution to (5) does not decay to zero. In order to avoid the exponential convergence to zero as $t \to \infty$, we have to choose $\Omega = I_v \times I_x$ such that the solution $\widetilde{f}$ is not decaying to zero. From the above expressions, it easily follows that in order to ensure this condition, we must have:

$$\begin{cases} |I_v| \geqslant \sqrt{2} & \text{if } |I_v| \leqslant |I_x|, \\ |I_x| \geqslant \sqrt{2} & \text{if } |I_v| > |I_x|. \end{cases}$$

That is to say, in any cases, $|I_v| \geqslant \sqrt{2}$ and $|I_x| \geqslant \sqrt{2}$. □

5. Discretization schemes

In this section, we introduce the numerical schemes used to solve the various forms of the Kolmogorov equations, i.e. eqs. (1) and (5). This is needed to compare the effectiveness of the self-similarity change of variables introduced in Section 3, which is discussed in Section 6.

Since eq. (1) and (5) are not coercive it is quite natural to use an operator splitting method. Thus, in this subsection we will introduce two operator splitting methods for the simulation of eqs. (1) and (5). The operator splitting method for (1) will be a second order scheme, while the method used for (5) will be an exact method.

In order to simulate the equation, we will truncate the solution to a bounded domain Ω of $\mathbb{R}^2$, as in Section 4. Then, the spatial approximation will be based on the finite element method. To this end, in this section, $\mathcal{T}^h$ is a triangulation of Ω with given average triangle size, h, and $X^h \subset H_0^1(\Omega)$ is the set of P_1-finite elements based on this triangulation $\mathcal{T}^h$. Let us also define P^h a projector of $H_0^1(\Omega)$ to X^h.

5.1. Operator splitting for Kolmogorov equation

As stated above the Kolmogorov equation, (1), is not coercive and thus an operator splitting method will be used in our simulations. The operator splitting method Algorithm 1 introduced in this subsection is second order accurate and thus some care must be taken when simulating over long times. Thus, we see that there is not only a problem with artificial boundary conditions, but the accuracy of the method tends to cause a problem.

For the operator splitting method used on the Kolmogorov equation, (1), we define two operators

$$\mathcal{A}_1 = \partial_t - \partial_v^2 \tag{13a}$$

$$\mathcal{A}_2 = \partial_t - v \, \partial_x. \tag{13b}$$

With these two operators in place we can solve the first operation using a finite element method, or some other method of choice, while solving the second operation using an exact solution from the method of characteristics.

To this end we introduce the following weak form relating to the operator $\mathcal{A}_1$. Given the test function $\chi \in H_0^1(\Omega)$ then the weak form for $\mathcal{A}_1$ defined on a domain $\Omega \subset \mathbb{R}^2$ with $f|_{\partial\Omega} = 0$ is

Find $f \in H_0^1(\Omega)$ such that

$$(\partial_t f, \chi) + (\partial_v f, \partial_v \chi) = 0 \quad \forall \chi \in H_0^1(\Omega) .$$

For the operator $\mathcal{A}_2$ the method of characteristics can be used and therefore it is easy to see that the solution of

$$\partial_t f - v \partial_x f = 0 \qquad \text{on } \Omega ,$$

$$f(\cdot, \cdot, 0) = f_0 \qquad \text{on } \Omega$$

is

$$f(v, x, t) = f_0(v, x + v t) \qquad (t \geqslant 0, \; (v, x) \in \Omega)$$

and so an exact solution can be obtained using a translation.

Using these two operators we then define Algorithm 1 for determining the solution to the Kolmogorov equation, (1), using finite elements.

Algorithm 1: Operator splitting method for Kolmogorov equation (1).

Given $\Delta t > 0$ a time step and given $f_0 \in H_0^1(\Omega)$.

initialization Set $f_h^0 = P^h f_0 \in X^h$.

repeat

1. Find $\varphi_h \in X^h$ such that

$$(\partial_t \varphi_h, \chi_h) + (\partial_v \varphi_h, \partial_v \chi_h) = 0 \qquad (t \in (0, \Delta t), \; \chi_h \in X^h),$$

$$\varphi_h(0) = f_h^n.$$

2. Using the method of characteristics solve

$$\partial_t \psi_h = v \partial_x \psi_h \qquad (t \in (0, \Delta t)),$$

$$\psi_h(0) = \varphi_h(\Delta t).$$

3. Update solution,

$$f_h^{n+1} = \psi_h(\Delta t).$$

until $n\Delta t = T$.

The proof of the convergence of Algorithm 1 can be found in [15].

5.2. An exact splitting scheme

The self-similar version of the Kolmogorov equation (5) is not coercive and so a unique solution to the finite element discretization is not guaranteed. To address this issue we can split the (5) into two operators. We will select these operators in such a way that both are coercive and commute, since operators which commute result in a no error from the operator splitting scheme. The following theorem states that there exists an operator splitting for (5) which is exact.

Proposition 5.1. *Set $\sigma_1 \leqslant 1$ and $\sigma_2 = 2 - \sigma_1$ and define*

$$K_{1,s} = -\left(\partial_{\widetilde{v}} + (1 - e^{-s})\partial_{\widetilde{x}}\right)^2 - \frac{1}{2}\widetilde{v}\partial_{\widetilde{v}} - \frac{3}{2}\widetilde{x}\partial_{\widetilde{x}} - \sigma_1 \mathrm{Id}, \tag{14a}$$

$$K_{2,s} = \sigma_2 \, \mathbf{I}. \tag{14b}$$

Then $K_{1,s}$ and $K_{2,s}$ commute, $K_{2,s}$ is coercive on $H_0^1(\Omega)$, $K_{1,s}$ is coercive on $L^2(\Omega)$ and (5) can be written as

$$\partial_s \widetilde{f} = -K_{1,s}\widetilde{f} + K_{2,s}\widetilde{f}. \tag{15}$$

Proof. Since $\sigma_1 + \sigma_2 = 2$, it is obvious that (5) can be written as (15).

Since $\sigma_2 = 2 - \sigma_1 > 0$ and $K_{2,s}$ is a multiple of identity, it is obvious that $K_{2,s}$ is coercive and $K_{2,s}$ and $K_{1,s}$ commute. Let us now check that $K_{1,s}$ is coercive. As in the proof of Proposition 4.1, we have for every $\widetilde{f} \in H_0^1(\Omega)$,

$$\int_\Omega \widetilde{f} K_{1,s}\widetilde{f} = \int_\Omega \left|\partial_{\widetilde{v}}\widetilde{f} + (1 - e^{-s})\partial_{\widetilde{x}}\widetilde{f}\right|^2 + (1 - \sigma_1)\int_\Omega |\widetilde{f}|^2 \geqslant \left\|\partial_{\widetilde{v}}\widetilde{f} + (1 - e^{-s})\partial_{\widetilde{x}}\widetilde{f}\right\|_{L^2(\Omega)}^2.$$

But, according to Lemma 4.1, for every $s \geqslant 0$, there exists $C_\Omega(1 - e^{-s}) > 0$ such that

$$\left\|\partial_{\widetilde{v}}\widetilde{f} + (1 - e^{-s})\partial_{\widetilde{x}}\widetilde{f}\right\|_{L^2(\Omega)}^2 \geqslant \frac{1}{C_\Omega(1 - e^{-s})}\left\|\widetilde{f}\right\|_{L^2(\Omega)}^2. \quad \square$$

Since (5) is not coercive we cannot guarantee the Finite Element solution to (5) is unique. However, since $K_{1,s}$ and $K_{2,s}$ commute, we can create an exact operator splitting method where our operators are coercive by choosing $\sigma_1 \leqslant 1$ and $\sigma_2 = 2 - \sigma_1$.

For the purpose of the numerical simulation, we introduce the following weak form, relating to the operator $\partial_s + K_{1,s}$.

Find $\widetilde{f} \in H_0^1(\Omega)$ such that

$$(\partial_t \widetilde{f}, \chi) + a_s(\widetilde{f}, \chi) = 0 \quad \forall \chi \in H_0^1(\Omega),$$

where we have set

$$a_s(\widetilde{f}, \chi) = (\partial_{\widetilde{v}} \widetilde{f}, \partial_{\widetilde{v}} \chi) + (1 - e^{-s})\left((\partial_{\widetilde{v}} \widetilde{f}, \partial_{\widetilde{x}} \chi) + (\partial_{\widetilde{x}} \widetilde{f}, \partial_{\widetilde{v}} \chi)\right) + (1 - e^{-s})^2 (\partial_{\widetilde{x}} \widetilde{f}, \partial_{\widetilde{x}} \chi)$$

$$+ \frac{1}{4}\left((\widetilde{f}, \widetilde{v} \partial_{\widetilde{v}} \chi) - (\widetilde{v} \partial_{\widetilde{v}} \widetilde{f}, \chi)\right) + \frac{3}{4}\left((\widetilde{f}, \widetilde{x} \partial_{\widetilde{x}} \chi) - (\widetilde{x} \partial_{\widetilde{x}} \widetilde{f}, \chi)\right)$$

$$+ (1 - \sigma_1)(\widetilde{f}, \chi).$$

For the operator $K_{2,s}$, the solution is explicit. In fact, it is easy to see that the solution of

$$\partial_s \widetilde{f} - K_{2,s} \widetilde{f} = 0 \qquad \text{on } \Omega,$$

$$f(\cdot, \cdot, 0) = f_0 \qquad \text{on } \Omega$$

is

$$f(\cdot, \cdot, s) = e^{\sigma_2 s} f_0 \qquad (s \geqslant 0).$$

Using these two operators we then define Algorithm 2 for determining the solution to the Kolmogorov equation in self-similar variables (5), using finite elements.

Algorithm 2: Operator splitting method for the self-similar Kolmogorov equation (5).

Given $\Delta s > 0$ a time step and given $f_0 \in H_0^1(\Omega)$.
initialization Set $\widetilde{f}_h^0 = P^h f_0 \in X^h$.
repeat
1.   Find $\varphi_h \in X^h$ such that

$$(\partial_t \varphi_h, \chi_h) + a_s(\varphi_h, \chi_h) = 0 \qquad (t \in (0, \Delta s), \ \chi_h \in X^h), \tag{16a}$$
$$\varphi_h(0) = \widetilde{f}_h^n. \tag{16b}$$

2.   Update solution,

$$f_h^{n+1} = e^{\sigma_2 \Delta s} \varphi_h(\Delta s).$$

until $n\Delta s = T$.

In the numerical test, we will use Crank–Nicolson method to solve (16).

6. Numerical results

In this section we compare the results of the finite element method applied to the various forms of the Kolmogorov Equation, eqs. (1) and (5). The comparison will be performed on two different initial conditions, eqs. (19) and (23). The first initial condition, (19), is a smooth Gaussian, while the second initial condition, (23), is a square pulse centered at zero. In this way, we demonstrate the benefits of using the self-similarity change of variables, which include

- Small space domain,
- Fast marching in time,
- Convergence to steady state.

In what follows we determine the effectiveness of each finite element discretization introduced in Section 5 through comparison of L^2-errors and a percent difference defined as

$$\%\mathrm{diff}(f) = \frac{\|f_{numerical} - f_{\mathrm{exact}}\|}{\|f_{\mathrm{exact}}\|} \cdot 100\%. \tag{17}$$

The use of %diff will show the distribution of error and thus show where the largest errors occur. For (1) the major contribution of errors is expected to occur on the boundary, due to the interaction with the artificial boundary conditions. However, it is expected that for the self-similarity solution of (5), the major contribution of error should directly come from discretization error rather than imposed boundary conditions.

For the various forms of the Kolmogorov Equation, eqs. (1) and (5), we take the time interval, and problem domain to be respectively

$$I = [0, 10], \quad \Omega = [-10, 10] \times [-10, 10], \tag{18}$$

Table 1
L^2-error for the finite element discretizations at $t = 10$ (i.e. $s = \ln(t - 1) = \ln(9)$ for Algorithm 2).

Algorithm 1	Algorithm 2
0.0490644	0.019473

which obviously satisfies condition (12). For each equation we take the time step to be $\Delta t = \Delta s = 0.01$ and the number of triangles along each side of the domain, Ω, to be $N = 128$.

Remark 6.1. We note that while the starting domain for (5) is given by Ω the respective change of variables results in the domain growing over time. Additionally, since s is a scaling of the time, t, we take the time interval for (5) to be $I_s = [0, 2.4]$ which corresponds to $t \in I$, since $t = e^s - 1 \Rightarrow s \in [0, \log(t + 1)]$.

Due to the scaling in time, when comparing solution behavior (L^2 and L^∞ norms) over time we will take $t \in [0, 240]$ for simulating the Kolmogorov Equation, (1). This will allow for a proper comparison of long time behavior in the norms. While $t = 240$ is still no where close to the final time of $s = 10$, we obtain a good picture of the decay rate over time. Running the simulation out to this time took quite a bit of computational time especially as compared to simulating, (5), out to $s = 10$.

To this end, we begin by comparing the simulations given an exact solution resulting from the initial condition (19). In the last subsection we will compare long time solution behavior given a square pulse as the initial condition. No finite element error analysis will be performed on this example, since we do not have an exact solution.

6.1. Test 1: simulation with exact solution

For the purposes of comparing solutions and contribution of errors from the finite element discretization we first need exact solutions to each of the different forms of the Kolmogorov Equation. To this end, we define the initial condition

$$f_0(v, x) = e^{-v^2 - x^2} \tag{19}$$

and therefore the solutions to eqs. (1) and (5) are respectively given by

$$f_{\text{exact}}(t, v, x) = \frac{\exp\left(-\frac{(3 + 3t^2 + 4t^3)v^2 + 6t(1 + 2t)vx + 3(1 + 4t)x^2}{3 + 12t + 4t^3 + 4t^4} \right)}{\sqrt{1 + 4t + \frac{4}{3}t^2 + \frac{4}{3}t^4}}, \tag{20}$$

$$\widetilde{f}_{\text{exact}}(s, v, x) = \frac{\exp\left(\frac{(1 - 4e^s(3 + e^s(-3 + e^s)))v^2 + 12e^s(-1 + e^s)^2 vz - 3e^{2s}(-3 + 4e^s)z^2}{-9 + 8e^s + 12e^{2s} - 12e^{3s} + 4e^{4s}} \right)}{\sqrt{-3 + \frac{8}{3}e^s + 4e^{2s} - 4e^{3s} + \frac{4}{3}e^{4s}}}. \tag{21}$$

Additionally, from Theorem 3.1 we see that the solution to (5) converges to

$$\widetilde{f}_\infty(\widetilde{v}, \widetilde{x}) = \frac{\sqrt{3}}{2} e^{-\widetilde{v}^2 + 3\widetilde{v}\widetilde{x} - 3\widetilde{x}^2} \tag{22}$$

which is an elliptic Gaussian having magnitude $\frac{\sqrt{3}}{2}$.

For (1) the support of the solution grows beyond the problem domain in the given time interval, I, and therefore the boundary conditions become more and more important as time increases until the solution, given by the finite element method, no longer approximates the true solution of the original problem. This can be seen in Fig. 4. Thus, as time increases the error becomes larger and larger, due to the divergence from the exact solution caused by the interaction of the boundary conditions. While (5) tends to a steady state with compact support in the domain Ω for the given time interval, therefore the approximation given by the finite element method remains valid throughout the simulated time and should provide a better approximation to the exact solution, as can be seen in Fig. 5.

Additionally, the L^2-error at time $t = 10$ is smaller for the self-similarity version of the Kolmogorov Equation, (5), as compared to the original Kolmogorov Equation, (1), as expected, as seen in Table 1. In fact, the L^2-error for the self-similarity version of the Kolmogorov Equation at $t = e^{10} - 1$, i.e. $s = 10$, is still smaller than the L^2-error associated with (1) at $t = 10$ and is

$$\|\widetilde{f}_{\text{exact}}(10, \widetilde{v}, \widetilde{x}) - \widetilde{f}(10, \widetilde{v}, \widetilde{x})\| = 0.0107995.$$

Thus, we see that the self-similarity solution performs much better over long times.

Table 2
L^2-errors for finite element method applied to the self-similar Kolmogorov equation, (5), at $s = 10$ with $dt = 0.01$.

h	L^2-error	Order
1.00000	6.27854×10^{-1}	–
0.50000	9.90501×10^{-2}	2.6642
0.25000	2.70934×10^{-2}	1.8702
0.12500	6.94450×10^{-3}	1.9640
0.06250	1.74641×10^{-3}	1.9915
0.03125	4.36256×10^{-4}	2.0011
0.01562	1.08071×10^{-4}	2.0132
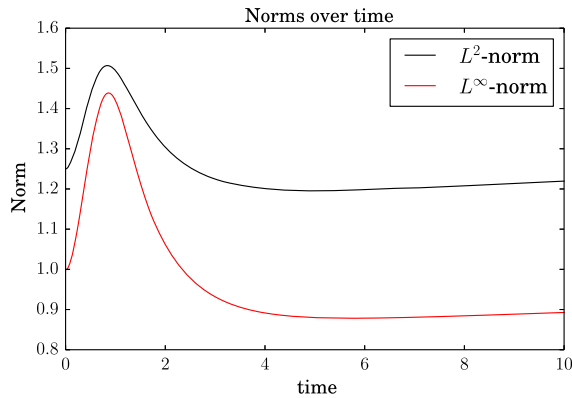
Fig. 2. The observed solution behavior over time for finite element method and Algorithm 2 applied to (5).
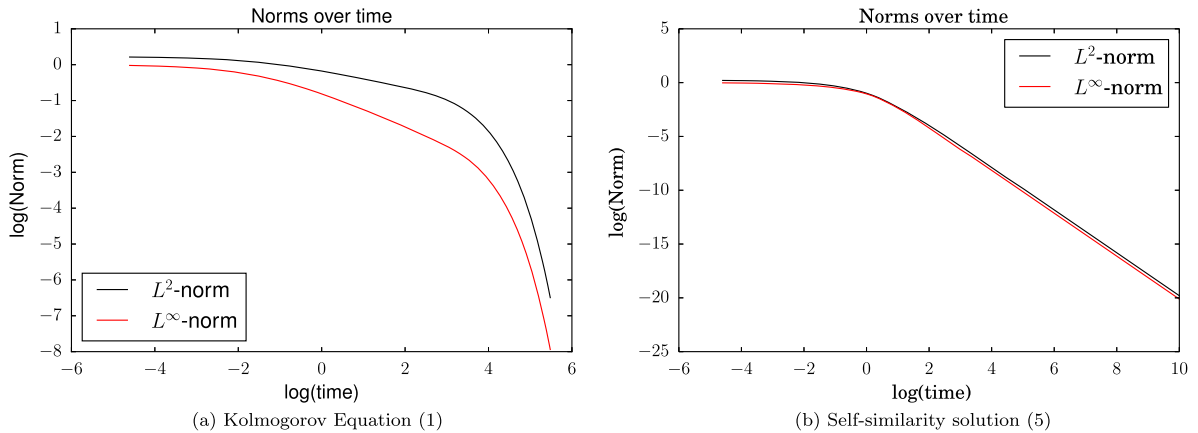
Fig. 3. Observed L^∞-norm and L^2-norm over time.

Remark 6.2 *(Finite element convergence).* We see in Table 2 that the rate of convergence appears to follow the classical quadratic convergence rate expected for linear finite elements and the convergence rate is given by the least squares fit

$$E(h) = 0.49796 \, h^{2.0401}.$$

In addition to the decreasing L^2-error for the finite element approximation to (5) we would like to bring the reader's attention back to behavior remarked in Proposition 3.1 relating to the L^∞-norm of (5) not being monotonic. Indeed, the numerical simulation of (5) by finite element method follows the same behavior as the one predicted by Proposition 3.1 and this can be seen in Fig. 2. In this simulation we observe that initially the L^∞-norm increases and then eventually decreases to a steady state as expected (see Fig. 2). We also note that while the graph appears to be increasing as time increases the data appears to be converging to a constant, and can be observed by the fact that the L^∞ eventually is only changing in the 4th decimal.

When comparing long time solution norms on a log–log (see Fig. 3a) plot we see that the solution given by Algorithm 2 applied to the Self-Similar Kolmogorov Equation seems to have a polynomial decay rate, while the solution given by Algorithm 1 applied to the Kolmogorov Equation seems to have a decay rate which is faster than any polynomial decay rate.
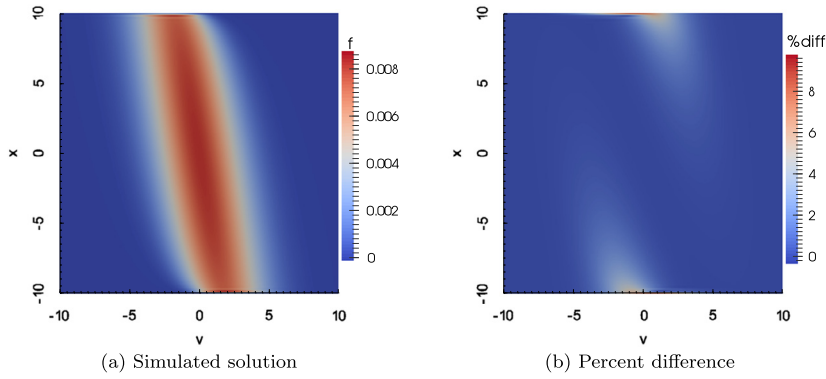
(a) Simulated solution

(b) Percent difference

Fig. 4. Solution to the Kolmogorov Equation, (1), simulated using Algorithm 1 (a) and percent difference (b) between exact solution and simulated solution at $t = 10$.
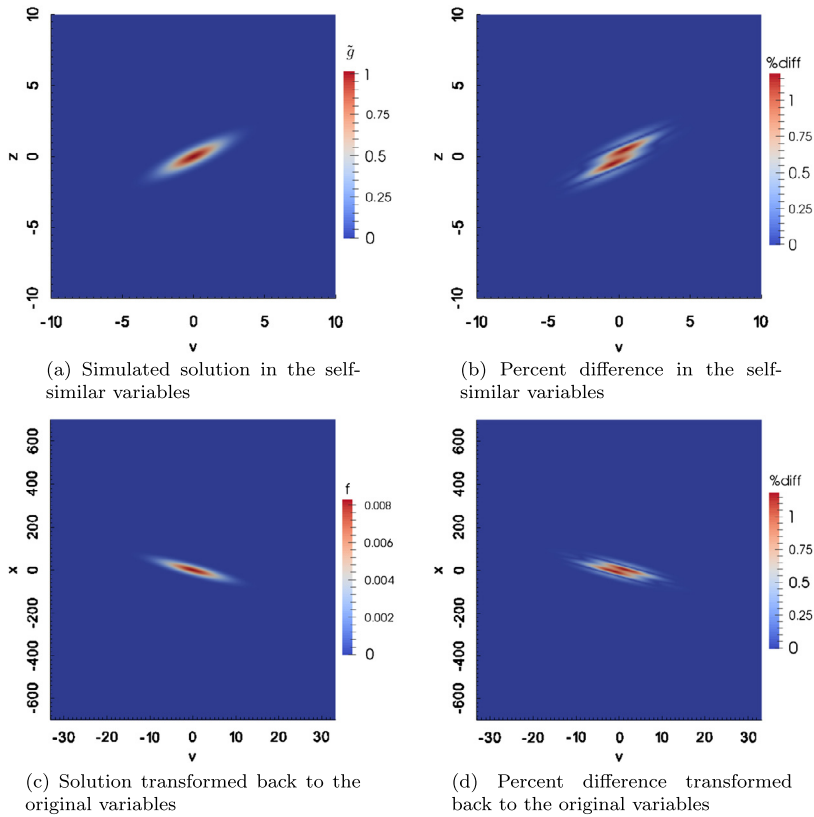

(a) Simulated solution in the self-similar variables

(b) Percent difference in the self-similar variables

(c) Solution transformed back to the original variables

(d) Percent difference transformed back to the original variables

Fig. 5. Solution to the self-similar Kolmogorov Equation, (5), using Algorithm 2 (a, c) and percent difference (b, d) between exact solution and simulated solution at $s = 2.40$ ($t \sim 10$).

Remark 6.3. We note that the change of variable $z = x + t\,v$ results in the rotation of the initial condition in the opposite direction to the direction seen in the original variables. This is apparent in both the exact solution given in (4) and the simulation presented in Section 6, especially in Fig. 5.

6.2. Test 2: square pulse

In the next example we take the initial condition to be a square pulse defined by

$$f(0, \mathbf{x}) = f_0(\mathbf{x}) = \begin{cases} 1 & \text{if } |x| < 1 \text{ and } |v| < 1 \\ 0 & \text{otherwise.} \end{cases} \tag{23}$$
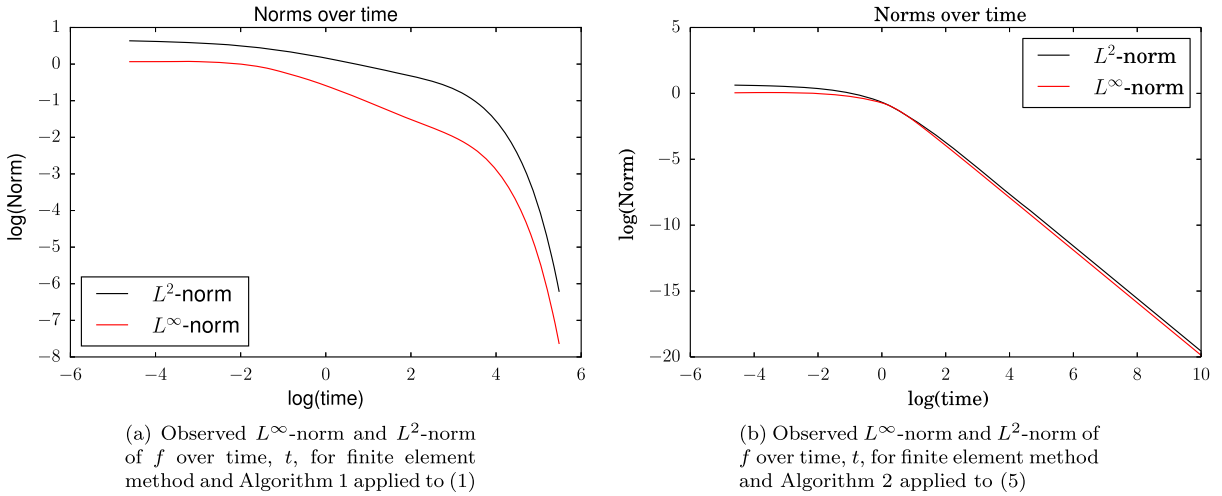
(a) Observed L^∞-norm and L^2-norm of f over time, t, for finite element method and Algorithm 1 applied to (1)

(b) Observed L^∞-norm and L^2-norm of f over time, t, for finite element method and Algorithm 2 applied to (5)

Fig. 6. Comparison of solution behavior over time for similarity solution, b, in original variables and Kolmogorov equation, a, with initial condition (23).
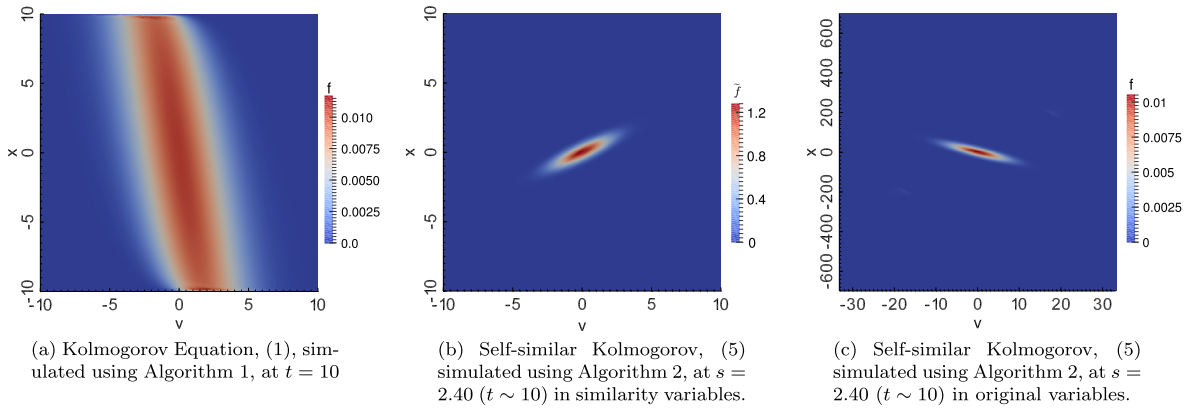

(a) Kolmogorov Equation, (1), simulated using Algorithm 1, at $t = 10$

(b) Self-similar Kolmogorov, (5) simulated using Algorithm 2, at $s = 2.40$ $(t \sim 10)$ in similarity variables.

(c) Self-similar Kolmogorov, (5) simulated using Algorithm 2, at $s = 2.40$ $(t \sim 10)$ in original variables.

Fig. 7. Comparison of solutions, at $t = 10$, to self-similar Kolmogorov, b and c, and Kolmogorov equations, a, with the initial condition (23).

For this initial condition we see that again the solution support has grown beyond the original domain size by $t = 10$ (see Fig. 7a), and therefore the boundary conditions begin to play a big role in the simulated solution. However, due to a lack of exact solution, we cannot quantify the error due to boundary conditions. However, we can determine the effects on the solution behavior.

The solution to the Kolmogorov Equation is supposed to follow a polynomial decay, but as can be seen in Fig. 6a the solution does not appear exhibit polynomial decay. However, in Fig. 6b, we see a clear trend of polynomial decay. In fact, polynomial decay which is of second order as indicated by the slope of the line in the log–log plot, Fig. 6b.

7. Conclusions

In this paper we introduce a discretization of the self-similar Kolmogorov equation (5) based on an operator splitting technique combined with a finite element method and provide theoretical results for the method. Then in Section 6 we verified our theoretical results. The effectiveness of the self-similar change of variables was demonstrated in Section 6, by comparing finite element solutions for (1) using the method of splitting in Algorithm 1, and the self-similar version of Kolmogorov (5). The self-similar change of variables had the lowest L^2-error as compared to the solutions for (1). The main reason for this was due to the interaction of the artificially imposed boundary conditions with the solution on the inside of the domain. This is exactly as expected. We note that the self-similar change of variables solution can also suffer from the same draw back of artificial boundary conditions if a domain which is too small is chosen. However, the key point here is that the domain required is much smaller than that of (1), allowing for efficient long time simulation. In addition to the ability to use much smaller domains for long time simulation, the self-similar change of variables allows for fast marching in time due to the change in time from t to s where $t = e^s - 1$. Thus, time marching is exponential which adds to the efficiency of computing solutions to the self-similar change of variables version of the Kolmogorov equation. In summary we see that for long time integration the self-similar change of variables has the following benefits, as compared to the original formulation of the Kolmogorov equation: small space domain, and fast marching in time.

Acknowledgements

Appendix A. Proof of Lemma 4.1

Let $g \in H_0^1(\Omega)$ and let us extend g by 0 outside Ω, so that $g \in H_0^1(I_v \times I_x)$. Assume that there exists $C_{I_v \times I_x}(t)$ such that

$$\|g\|_{L^2(I_v \times I_x)}^2 \leqslant C_{I_v \times I_x}(t)\|\partial_v g + t\partial_x g\|_{L^2(I_v \times I_x)}^2 .$$

But we have

$$\|g\|_{L^2(I_v \times I_x)}^2 = \|g\|_{L^2(\Omega)}^2 \quad \text{and} \quad \|\partial_v g + t\partial_x g\|_{L^2(I_v \times I_x)}^2 = \|\partial_v g + t\partial_x g\|_{L^2(\Omega)}^2 .$$

Consequently, for every $g \in H_0^1(\Omega)$, there exists $C_\Omega(t) \leqslant C_{I_v \times I_x}(t)$ so that

$$\|g\|_{L^2(\Omega)}^2 \leqslant C_\Omega(t)\|\partial_v g + t\partial_x g\|_{L^2(\Omega)}^2 .$$

Consequently, it remains to prove the existence and the estimate on $C_{I_v \times I_x}(t)$.

Assume now that $\Omega = I_v \times I_x$, with $I_v = (a_v, b_v)$ and $I_x = (a_x, b_x)$ and let $g \in H_0^1(I_v \times I_x)$. Let us define

$$\widetilde{g}(\widetilde{v}, \widetilde{x}) = g(a_v + (b_v - a_v)\widetilde{v}, a_x + (b_x - a_x)\widetilde{x}) \qquad ((\widetilde{v}, \widetilde{x}) \in (0,1)^2) .$$

Then we have $\widetilde{g} \in H_0^1((0,1)^2)$,

$$(\partial_{\widetilde{v}}\widetilde{g} + t\partial_{\widetilde{x}}\widetilde{g})(\widetilde{v}, \widetilde{x}) = |I_v|\left(\partial_v g + \frac{|I_x|}{|I_v|}t\partial_x g\right)(a_v + |I_v|\widetilde{v}, a_x + |I_x|\widetilde{x})$$

and

$$\|\widetilde{g}\|_{L^2((0,1)^2)}^2 = |I_v||I_x|\|g\|_{L^2(I_v \times I_x)}^2 \quad \text{and} \quad \|\partial_{\widetilde{v}}\widetilde{g} + t\partial_{\widetilde{x}}\widetilde{g}\|_{L^2((0,1)^2)}^2 = |I_v|^3|I_x|\left\|\partial_v g + \frac{|I_x|}{|I_v|}t\partial_x g\right\|_{L^2(I_v \times I_x)}^2 .$$

Consequently, if there exists $C_{(0,1)^2}(t)$ such that

$$\|g\|_{L^2((0,1)^2)}^2 \leqslant C_{(0,1)^2}(t)\|\partial_v g + t\partial_x g\|_{L^2((0,1)^2)}^2 \qquad (g \in H_0^1((0,1)^2)),$$

then,

$$\|g\|_{L^2(I_v \times I_x)}^2 \leqslant |I_v|^2 C_{(0,1)^2}\left(\frac{|I_v|}{|I_x|}t\right)\|\partial_v g + t\partial_x g\|_{L^2(I_v \times I_x)}^2 \qquad (g \in H_0^1(I_v \times I_x)) .$$

Consequently, it remains to prove the result for $\Omega = (0,1)^2$.

Let us prove the result for $g \in C_0^\infty(\Omega)$ (with $\Omega = (0,1)^2$), the global result will follow from density arguments. Let us extend g by 0 outside Ω, then we have $g \in C_c^\infty(\mathbb{R}^2)$. For every $(v_0, x_0) \in \mathbb{R}^2$ and every $s \in \mathbb{R}$, we have:

$$g(v_0 + s, x_0 + ts) = \int_0^s \frac{\mathrm{d}}{\mathrm{d}\sigma} g(v_0 + \sigma, x_0 + t\sigma)\,\mathrm{d}\sigma$$

$$= \int_0^s (\partial_v g(v_0 + \sigma, x_0 + t\sigma) + t\partial_x g(v_0 + \sigma, x_0 + t\sigma))\,\mathrm{d}\sigma .$$

Hence, by Cauchy–Schwarz inequality,

$$|g(v_0 + s, x_0 + ts)|^2 \leqslant s \int_0^s |\partial_v g(v_0 + \sigma, x_0 + t\sigma) + t\partial_x g(v_0 + \sigma, x_0 + t\sigma)|^2\,\mathrm{d}\sigma . \tag{24}$$

Before continuing, let us consider the particular case $t = 0$.
In this case, eq. (24) is

$$|g(v_0 + s, x_0)|^2 \leqslant s \int_0^s |\partial_v g(v_0 + \sigma, x_0)|^2 \, d\sigma$$

and hence,

$$\|g\|_{L^2(\Omega)}^2 = \int_0^1 \int_0^1 |g(v,x)|^2 \, dv dx \leqslant \int_0^1 \int_0^1 v \int_0^v |\partial_v g(\sigma, x)|^2 \, d\sigma \, dv dx$$

$$\leqslant \int_0^1 \int_0^1 v \int_0^1 |\partial_v g(\sigma, x)|^2 \, d\sigma \, dv dx \leqslant \frac{1}{2} \|\partial_v g\|_{L^2(\Omega)}^2 .$$

That is to say $C_\Omega(0) \leqslant \frac{1}{2}$.

Let us now consider the case $t > 0$. Then, we have

$$\|g\|_{L^2(\Omega)}^2 = \int_0^1 \int_0^1 |g(v,x)|^2 \, dx dv = t \int_0^1 \int_0^{\frac{1}{t}} |g(v,ts)|^2 \, ds dv = t \int_0^{\frac{1}{t}} \int_{-s}^{1-s} |g(w+s,ts)|^2 \, dw ds .$$

Then,

- if $t < 1$,

$$\|g\|_{L^2(\Omega)}^2 = t \left(\int_{\frac{-1}{t}}^{1-\frac{1}{t}} \int_{-w}^{\frac{1}{t}} |g(w+s,ts)|^2 \, ds dw + \int_{1-\frac{1}{t}}^{0} \int_{-w}^{1-w} |g(w+s,ts)|^2 \, ds dw + \int_0^1 \int_0^{1-w} |g(w+s,ts)|^2 \, ds dw \right) ;$$

- if $t \geqslant 1$,

$$\|g\|_{L^2(\Omega)}^2 = t \left(\int_{\frac{-1}{t}}^{0} \int_{-w}^{\frac{1}{t}} |g(w+s,ts)|^2 \, ds dw + \int_0^{1-\frac{1}{t}} \int_0^{\frac{1}{t}} |g(w+s,ts)|^2 \, ds dw + \int_{1-\frac{1}{t}}^1 \int_0^{1-w} |g(w+s,ts)|^2 \, ds dw \right) .$$

All the integrals in the above expressions are of the form:

$$\int_a^b \int_{\alpha(w)}^{\beta(w)} |g(w+s,ts)|^2 \, ds \, dw,$$

with $a \leqslant b$ and $\alpha(w) \leqslant \beta(w)$.

But we have, using eq. (24),

$$\int_a^b \int_{\alpha(w)}^{\beta(w)} |g(w+s,ts)|^2 \, ds dw$$

$$= \int_a^b \int_0^{\beta(w)-\alpha(w)} |g(w+\alpha(w)+s, ts+t\alpha(w))|^2 \, ds dw$$

$$\leqslant \int_a^b \int_0^{\beta(w)-\alpha(w)} s \int_0^s |\partial_w g(w+\alpha(w)+\sigma, t\sigma+t\alpha(w)) + t\partial_x g(w+\alpha(w)+\sigma, t\sigma+t\alpha(w))|^2 \, d\sigma \, ds dw$$

$$\leqslant \int_a^b \int_0^{\beta(w)-\alpha(w)} s \int_{\alpha(w)}^{s+\alpha(w)} |\partial_w g(w+\sigma, t\sigma) + t\partial_x g(w+\sigma, t\sigma)|^2 \, d\sigma \, ds dw$$

$$\leqslant \int_a^b \int_0^{\beta(w)-\alpha(w)} s \int_{\alpha(w)}^{\beta(w)} |\partial_w g(w+\sigma, t\sigma) + t\partial_x g(w+\sigma, t\sigma)|^2 \, d\sigma \, ds dw$$

$$\leqslant \int_a^b \frac{(\beta(w) - \alpha(w))^2}{2} \int_{\alpha(w)}^{\beta(w)} |\partial_w g(w + \sigma, t\sigma) + t\partial_x g(w + \sigma, t\sigma)|^2 \, d\sigma \, dw$$

$$\leqslant \frac{1}{2} \left(\sup_{w \in [a,b]} (\beta(w) - \alpha(w))^2 \right) \int_a^b \int_{\alpha(w)}^{\beta(w)} |\partial_w g(w + \sigma, t\sigma) + t\partial_x g(w + \sigma, t\sigma)|^2 \, d\sigma \, dw.$$

Consequently,

- if $0 < t < 1$,

$$\|g\|_{L^2(\Omega)}^2 \leqslant \frac{t}{2} \left(\int_{\frac{-1}{t}}^{1-\frac{1}{t}} \int_{-w}^{\frac{1}{t}} |\partial_w g(w + s, ts) + t\partial_x g(w + s, ts)|^2 \, ds \, dw \right.$$

$$+ \int_{1-\frac{1}{t}}^0 \int_{-w}^{1-w} |\partial_w g(w + s, ts) + t\partial_x g(w + s, ts)|^2 \, ds \, dw$$

$$\left. + \int_0^1 \int_0^{1-w} |\partial_w g(w + s, ts) + t\partial_x g(w + s, ts)|^2 \, ds \, dw \right);$$

- if $t \geqslant 1$,

$$\|g\|_{L^2(\Omega)}^2 = \frac{1}{2t} \left(\int_{\frac{-1}{t}}^0 \int_{-w}^{\frac{1}{t}} |\partial_w g(w + s, ts) + t\partial_x g(w + s, ts)|^2 \, ds \, dw \right.$$

$$+ \int_0^{1-\frac{1}{t}} \int_0^{\frac{1}{t}} |\partial_w g(w + s, ts) + t\partial_x g(w + s, ts)|^2 \, ds \, dw$$

$$\left. + \int_{1-\frac{1}{t}}^1 \int_0^{1-w} |\partial_w g(w + s, ts) + t\partial_x g(w + s, ts)|^2 \, ds \, dw \right).$$

Going back to $[0, 1]^2$, we end up with

$$\|g\|_{L^2(\Omega)}^2 \leqslant \begin{cases} \frac{1}{2} \|\partial_w g + t\partial_x g\|_{L^2(\Omega)}^2 & \text{if } 0 < t \leqslant 1, \\ \frac{1}{2t^2} \|\partial_w g + t\partial_x g\|_{L^2(\Omega)}^2 & \text{if } t > 1. \end{cases}$$

All in all, we have proved that $C_{(0,1)^2}(t)$ exists and we have

$$C_{(0,1)^2}(t) \leqslant \begin{cases} \frac{1}{2} & \text{if } 0 \leqslant t \leqslant 1, \\ \frac{1}{2t^2} & \text{if } t \geqslant 1 \end{cases} \qquad (t \geqslant 0). \quad \square$$

References

[1] K. Beauchard, E. Zuazua, Some controllability results for the 2D Kolmogorov equation, Ann. Inst. Henri Poincaré, Anal. Non Linéaire 26 (5) (2009) 1793–1815.
[2] M. Berger, R.V. Kohn, A rescaling algorithm for the numerical calculation of blowing-up solutions, Commun. Pure Appl. Math. 41 (6) (1988) 841–863.
[3] M. Bessemoulin-Chatard, A finite volume scheme for convection–diffusion equations with nonlinear diffusion derived from the Scharfetter–Gummel scheme, Numer. Math. 121 (4) (2012) 637–670.
[4] M. Bessemoulin-Chatard, F. Filbet, A finite volume scheme for nonlinear degenerate parabolic equations, SIAM J. Sci. Comput. 34 (5) (2012) B559–B583.

[5] C.J. Budd, G.J. Collins, V.A. Galaktionov, An asymptotic and numerical description of self-similar blow-up in quasilinear parabolic equations, J. Comput. Appl. Math. 97 (1–2) (1998) 51–80.

[6] C. Buet, K.-C. Le Thanh, About positive, energy conservative and equilibrium state preserving schemes for the isotropic Fokker–Planck–Landau equation, preprint.

[7] O. Calin, D.-C. Chang, H. Fan, The heat kernel for Kolmogorov type operators and its applications, J. Fourier Anal. Appl. 15 (6) (2009) 816–838.

[8] C. Chainais-Hillairet, F. Filbet, Asymptotic behaviour of a finite-volume scheme for the transient drift-diffusion model, IMA J. Numer. Anal. 27 (4) (2007) 689–716.

[9] J. Chang, G. Cooper, A practical difference scheme for Fokker–Planck equations, J. Comput. Phys. 6 (1) (1970) 1–16.

[10] M. Escobedo, E. Zuazua, Self-similar solutions for a convection–diffusion equation with absorption in $\mathbf{R}^N$, Isr. J. Math. 74 (1) (1991) 47–64.

[11] M. Escobedo, E. Zuazua, Long-time behavior for a convection–diffusion equation in higher dimensions, SIAM J. Math. Anal. 28 (3) (1997) 570–594.

[12] A. Fiebach, A. Glitzky, A. Linke, Uniform global bounds for solutions of an implicit Voronoi finite volume method for reaction–diffusion problems, Numer. Math. 128 (1) (2014) 31–72.

[13] F. Filbet, T. Rey, A rescaling velocity method for dissipative kinetic equations. Applications to granular media, J. Comput. Phys. 248 (2013) 177–199.

[14] F. Filbet, G. Russo, A rescaling velocity method for kinetic equations: the homogeneous case, in: Modelling and Numerics of Kinetic Dissipative Systems, ISBN 1-59454-503-0, Nova Science, Hauppauge, NY, 2006, pp. 191–202.

[15] L. Gerardo-Giorda, M.B. Tran, Parallelizing the Kolmogorov–Fokker–Planck equation, ESAIM: Math. Model. Numer. Anal. 10 (2014), eFirst.

[16] A. Glitzky, Uniform exponential decay of the free energy for Voronoi finite volume discretized reaction–diffusion systems, Math. Nachr. 284 (17–18) (2011) 2159–2174.

[17] L. Hörmander, Hypoelliptic second order differential equations, Acta Math. 119 (1967) 147–171.

[18] W. Huang, J. Ma, R.D. Russell, A study of moving mesh PDE methods for numerical simulation of blowup in reaction diffusion equations, J. Comput. Phys. 227 (13) (2008) 6532–6552.

[19] A. Kolmogoroff, Zufällige Bewegungen (zur Theorie der Brownschen Bewegung), Ann. of Math. (2) 35 (1) (1934) 116–117.

[20] N.R. Nassif, N. Makhoul-Karam, Y. Soukiassian, Computation of blowing-up solutions for second-order differential equations using re-scaling techniques, J. Comput. Appl. Math. 227 (1) (2009) 185–195.

[21] R. Plato, Large time asymptotics for a fully discretized Fokker–Planck type equation, preprint.

[22] A. Porretta, E. Zuazua, Numerical hypocoercivity for the Kolmogorov equation, Math. Comput. 86 (303) (2017) 97–119, http://dx.doi.org/10.1090/mcom/3157.

[23] F. Rossi, Large time behavior for the heat equation on Carnot groups, Nonlinear Differ. Equ. Appl. 20 (3) (2013) 1393–1407.

[24] R.D. Russell, J.F. Williams, X. Xu, MOVCOL4: a moving mesh code for fourth-order time-dependent partial differential equations, SIAM J. Sci. Comput. 29 (1) (2007) 197–220 (electronic).

[25] C. Villani, Hypocoercive diffusion operators, in: International Congress of Mathematicians, vol. III, Eur. Math. Soc., Zürich, 2006, pp. 473–498.